# A Room Temperature Direct Metal Insertion into a Nonstrained Carbon−Carbon Bond in Solution. C−C vs C−H Bond Activation

**Boris Rybtchinski, Arkadi Vigalok, Yehoshoa Ben-David, and David Milstein***

*Contribution from the Department of Organic Chemistry, The Weizmann Institute of Science, Rehovot 76100, Israel*

*Received July 2, 1996*[⊗]

**Abstract:** The diphosphine 1,3-bis[(di-*tert*-butylphosphino)methyl]-2,4,6-trimethylbenzene (**1a**) upon reacting with the rhodium and iridium olefin complexes $M_2(olefin)_4Cl_2$ (M = Rh, Ir) undergoes rapid, selective metal insertion into the strong unstrained aryl−methyl bond under very mild conditions (room temperature), yielding $ClM(CH_3)$-$[C_6H(CH_3)_2(CH_2P(t\text{-}Bu)_2)_2]$ (M = Rh (**4a**), Ir (**7a**)). The carbon−carbon bond activation is competitive with a parallel C−H activation process, which results in formation of complexes $ClMH(L)[CH_2C_6H(CH_3)_2(CH_2P(t\text{-}Bu)_2)_2]$ (M = Rh (**3a**), Ir (**6a**); L = cyclooctene in the case of **6a** and is absent in **3a**). Complexes **3a** and **6a** undergo facile C−H reductive elimination (at room temperature (**3a**) or upon moderate heating (**6a**)), followed by C−C oxidative addition, resulting in clean formation of **4a** and **7a**, respectively. The C−C bond activation products are stable under the reaction conditions, demonstrating that this process is the thermodynamically favorable one. X-ray single-crystal analysis of **4a** demonstrates that the rhodium atom is located in the center of a square pyramid, with the methyl group occupying the position trans to the vacant coordination site. Direct kinetic comparison of the C−C and C−H activation processes shows that—in contrast to theoretical calculations—metal insertion into the carbon−carbon bond in this system is not only thermodynamically but also kinetically preferred over the competing insertion into the carbon−hydrogen bond. When the ligand 1,3-bis[(di-*tert*-butylphosphino)methyl]-2,4,6-trimethyl-5-methoxybenzene (**1b**), bearing the strong electron-donating methoxy group in the position *trans* to the $Ar-CH_3$ bond to be cleaved, was used instead of **1a**, no effect on the reaction rate or on the ratio between the C−H and C−C activation products was observed. Our observations indicate that the C−C oxidative addition proceeds via a three-centered mechanism involving a nonpolar transition state, similar to the one proposed for C−H activation of hydrocarbons. An $\eta^2$-arene complex is not involved in the C−C activation process.

## Introduction

Metal-complex-promoted activation of C−H and C−C bonds in homogeneous media is among the most important fields in organometallic chemistry, since it can lead to the design of new selective and efficient processes for utilization of hydrocarbons. While C−H activation in solution, forming products of metal insertion into C−H bonds, has been extensively studied,[1] examples of C−C oxidative addition by soluble metal complexes are less common, and this area is of much current interest.[2−4] Metal insertion into C−C bonds is believed to be both kinetically and thermodynamically less favorable than the competing C−H insertion.[1a,b] Kinetic factors, e.g., ease of a metal center approach to a C−H bond vs a C−C bond, statistical abundance of the C−H bonds, and an expected substantially higher activation energy for the C−C oxidative addition step itself, generally drive the bond activation processes toward C−H activation.[1a] In order to render the process of C−C insertion thermodynamically more favorable, an extra driving force is normally required, such as strain relief,[2a−g] the drive to aromaticity in prearomatic systems,[2h−l] or the presence of an activating functionality, such as a carbonyl group.[2m−p] Carbon−carbon bond cleavage of cyclopentadiene on a ruthenium hydride cluster[2q] and of agostic cations formed by protonation of cobalt diene complexes[2r] were recently observed.

We have recently demonstrated that a late transition metal center is capable of insertion into an unstrained, strong carbon−carbon bond in solution.[3,4] Although C−H bond activation takes place initially, C−C bond cleavage can be quantitatively accomplished by using hydrogen or methylene group "acceptors". We have also communicated that, upon heating at 150 °C, direct rhodium insertion into a carbon−carbon bond

[⊗] Abstract published in *Advance ACS Abstracts,* November 15, 1996.

(1) For example see: (a) Crabtree, R. H. In *The Chemistry of Alkanes and Cycloalkanes*; Patai, S., Rappoport, Z., Eds.; John Wiley & Sons: New York, 1992; p 653. (b) Crabtree, R. H. *Chem. Rev.* **1985**, *85*, 245. (c) Arndtsen, B. A.; Bergman, R. G.; Mobley, T. A.; Peterson, T. H. *Acc. Chem. Res.* **1995**, *28,* 154.

(2) (a) Adams, D. M.; Chatt, J.; Guy, R.; Sheppard, N. *J. Chem. Soc.* **1961**, 738. (b) Periana, R. A.; Bergman, R. G. *J. Am. Chem. Soc.* **1986**, *108*, 7346. (c) Hemond, R. C.; Hughes, R. P.; Robinson, D. J.; Rheingold, A. L. *Organometallics* **1988**, *7*, 2239. (d) Hughes, R. P.; Trujillo, H. A.; Rheingold, A. L. *J. Am. Chem. Soc.* **1993**, *115*, 1583. (e) Perthuisot, C.; Jones, W. D. *J. Am. Chem. Soc.* **1994**, *116*, 3647. (f) Li, R. T.; Nguyen, S. T.; Grubbs, R. H.; Ziller, J. W. *J. Am. Chem. Soc.* **1994**, *116*, 10032. (g) Lu, Z.; Jun, C.-L.; de Gala, S.; Sigalas, M. P.; Eisenstein, O.; Crabtree, R. H. *Organometallics* **1994**, *114*, 1168. (h) Crabtree, R. H.; Dion, R. P.; Gibboni, D. J.; McGrath, D. V.; Holt, E. M. *J. Am. Chem. Soc.* **1986**, *108*, 7222. (i) Kang, J. W.; Moseley, R.; Maitlis, P. M. *J. Am. Chem. Soc.* **1969**, *91*, 5970. (j) Benfield, F. W. C.; Green, M. L. H. *J. Chem. Soc., Dalton Trans.* **1974**, 1324. (k) Eilbracht, P. *Chem. Ber.* **1980**, *113*, 542. (l) Hemond, R. C.; Hughes, R. P.; Locker, M. B. *Organometallics* **1986**, *5*, 2392. (m) Suggs, J. W.; Jun, C.-H. *J. Am. Chem. Soc.* **1984**, *106*, 3054. (n) *Ibid.* **1986**, *108*, 4679. (o) Hartwig, J. F.; Anderson, R. A.; Bergman, R. G. *J. Am. Chem. Soc.* **1989**, *111*, 2717. (p) Murakami, M.; Amii, H.; Ito, Y. *Nature* **1994**, *370*, 540. (q) Suzuki, H.; Takaya, Y.; Takemori, T. *J. Am. Chem. Soc.* **1994**, *116*, 10779. (r) Nicholls, J. C.; Spencer, J. L. *Organometallics* **1994**, *13*, 1781.

(3) (a) Gozin, M.; Weisman, A.; Ben-David, Y.; Milstein, D. *Nature* **1993**, *364*, 699. (b) Gozin, M.; Aizenberg, M.; Liou, Sh.-Y.; Weisman, A.; Ben-David, Y.; Milstein, D. *Nature* **1994**, *370*, 42.

(4) (a) Liou, Sh.-Y.; Gozin, M.; Milstein, D. *J. Am. Chem. Soc.* **1995**, *117*, 9774. (b) Liou, Sh.-Y.; Gozin, M.; Milstein, D. *J. Chem. Soc., Chem. Commun.* **1995**, 1965. (c) van der Boom, M. E.; Kraatz, H.-B.; Ben-David, Y.; Milstein, D. *J. Chem. Soc., Chem. Commun.* **1996**, 2167.

S0002-7863(96)02253-6 CCC: $12.00 

**Scheme 1**

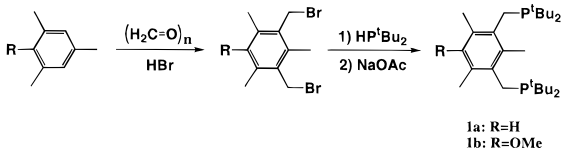


**Scheme 2**

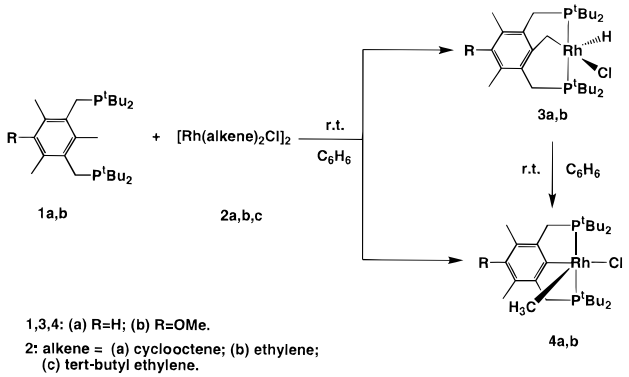


occurs.[4a] Here we report, for the first time, a reaction system in which *direct metal insertion* into a strong, unstrained C−C bond takes place at *room temperature*. Moreover, our system allows the thermodynamics and kinetics of the C−C and C−H bond activation processes to be compared directly, providing, for the first time, mechanistic information regarding oxidative addition of an unstrained C−C bond in solution.

## Results and Discussion

**Ligand Synthesis.** Bulky phosphines are advantageous ligands for the study of oxidative addition processes, especially cyclometalation, since upon coordination to a metal center they generate a species having a shielded vacant coordination site and a congested conformation. The latter assists the cyclometalation process due to favorable entropy.[5] In order to investigate the C−C and C−H bond activation processes, we synthesized the new diphosphine ligands DTBPM (**1a**) (2,4-bis[(di-*tert*-butylphosphino)methyl]mesitylene, 1,3-bis[(di-*tert*-butylphosphino)methyl]-2,4,6-trimethylbenzene) and DTBPA (**1b**) (3,5-bis[(di-*tert*-butylphosphino)methyl]-2,4,6-trimethylanisole, 1,3-bis[(di-*tert*-butylphosphino)methyl]-2,4,6-trimethyl-5-methoxybenzene), using bromomethylation[6a] followed by phosphination[6b] (Scheme 1). It should be noted that bromomethylation of mesitylene[6a] is a useful route for preparation of precursors in phosphine synthesis, resulting in high yields and good selectivity.

**C−C and C−H Bond Activation by Rhodium.** Remarkably, when a benzene solution of the dimeric rhodium olefin complex $[Rh(COE)_2Cl]_2$ (**2a**, COE = cyclooctene) and the ligand **1a** was stirred for 24 h at *room temperature*, direct rhodium insertion into one of the strong aryl−carbon bonds took place, yielding complex **4a** (Scheme 2). This complex was unambiguously characterized by various NMR techniques. The $^{31}P\{^1H\}$ NMR spectrum of **4a** exhibits a doublet at 57.37 ppm ($^1J_{RhP}$ = 118.9 Hz). The inequivalence of the Ar−$\mathbf{CH_2}$−Rh methylene protons in $^1H$ NMR and of the tertiary butyls in $^1H$ NMR and $^{13}C\{^1H\}$ NMR of **4a** indicate that there is no symmetry plane passing through the Rh−PCP chelate core. In $^1H$ NMR the Rh−$\mathbf{CH_3}$ group gives rise to a triplet of doublets positioned at 1.67 ppm ($^2J_{RhH}$ = 2.9 Hz, $^3J_{PH}$ = 4.9 Hz), which collapses to a doublet in $^1H\{^{31}P\}$ NMR. The Rh−$\mathbf{CH_3}$ group appears in $^{13}C\{^1H\}$ NMR as a doublet of triplets at 1.45 ppm ($^1J_{RhC}$ = 30.7 Hz and $^2J_{PC}$ = 5.9 Hz). The ipso-carbon of the Rh−**Ar** group gives rise to a doublet of triplets at 168.80 ppm ($^1J_{RhC}$ = 34.0 Hz and $^2J_{PC}$ = 5.9 Hz), confirming that in **4a** the rhodium atom is bound directly to the aryl ring. The structure of **4a** was confirmed by X-ray crystallography.

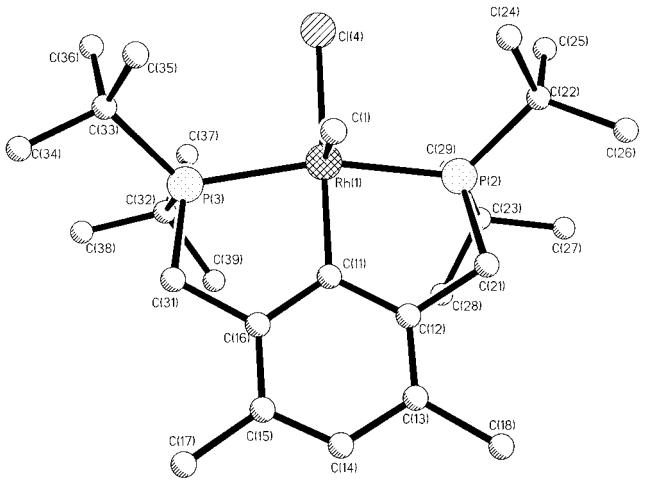


**Figure 1.** Perspective view of a molecule of Rh(DTBPM)($CH_3$)Cl (**4a**). Hydrogen atoms are omitted for clarity.

**Table 1.** Selected Bond Lengths (Å) and Bond Angles (deg) for **4a**

| | | | |
|---|---|---|---|
| Rh(1)−C(1) | 2.17(2) | Rh(1)−P(3) | 2.333(5) |
| Rh(1)−C(11) | 2.02(2) | Rh(1)−Cl(4) | 2.470(4) |
| Rh(1)−P(2) | 2.298(5) | | |
| C(11)−Rh(1)−C(1) | 80.3(8) | C(11)−Rh(1)−Cl(4) | 179.1(5) |
| C(11)−Rh(1)−P(2) | 83.8(5) | C(1)−Rh(1)−Cl(4) | 100.5(7) |
| C(1)−Rh(1)−P(2) | 91.8(6) | P(2)−Rh(1)−Cl(4) | 95.8(2) |
| C(11)−Rh(1)−P(3) | 82.8(5) | P(3)−Rh(1)−Cl(4) | 97.5(2) |
| P(2)−Rh(1)−P(3) | 164.6(2) | | |

**X-ray Crystallographic Study of 4a.** Orange prismatic crystals of complex **4a** were obtained upon crystallization from hexane at −30 °C. The single-crystal X-ray analysis demonstrates that the rhodium atom is located in the center of a square pyramid. The chloride ligand occupies the position *trans* to the ipso-carbon, whereas the methyl group is *trans* to the empty coordination site. A perspective view of a molecule of **4a** is shown in Figure 1. Selected bond lengths and bond angles are given in Table 1.

Other structural examples of late transition metal complexes based on PCP type ligands, bearing an apical methyl group in a square pyramidal configuration, have not been reported. The structure of **4a** is similar to that of the hydrido chloride complex Rh(H){2,6-($CH_2P$-*t*-$Bu_2$)$_2C_6H_3$}Cl,[7] in which the hydride is *trans* to the empty coordination site. The Rh(1)−P(2), Rh(1)−P(3), Rh−C(11), and Rh(1)−Cl(1) bond lengths in the chelate core of **4a** are similar to those reported for the hydrido chloride complex. Reported rhodium−methyl bond lengths in other square pyramidal rhodium complexes in which the methyl group is *trans* to an empty coordination site[8] are 2.081(9) Å (*trans*-Rh(Me)($PPh_3$)$_2I_2$),[8a] 2.031(6) Å (Rh(Me)(octaethylporphinate)),[8b]

(5) Shaw, B. L. *J. Organomet. Chem.* **1980**, *200*, 307.

(6) (a) Bromomethylation: van der Made, A. W.; van der Made, R. H. *J. Org. Chem.* **1993**, *58*, 1262. (b) Phosphine synthesis: Moulton, C. J.; Shaw, B. L. *J. Chem. Soc., Dalton Trans.* **1976**, 1020.

(7) Nemeh, S.; Jensen, C.; Binamira-Soriaga, E.; Kaska, W. C. *Organometallics* **1983**, *2*, 1442.

(8) (a) Troughton, P. G. H.; Skapski, A. C. *J. Chem. Soc., Chem. Commun.* **1968**, 575. (b) Takenaka, A.; Syal, S. K.; Sasada, Y.; Omura, T.; Ogoshi, H.; Yoshida, Z.-I. *Acta Crystallogr.* **1976**, *B32*, 62. (c) van der Zeijden, A. A. H.; van Koten, G.; Ernsting, J. M.; Elsevier, C. J.; Krijnen, B.; Stam, C. H. *J. Chem. Soc., Dalton Trans.* **1989**, 317.

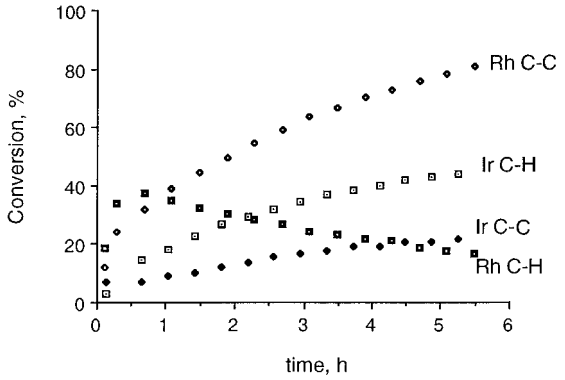


**Figure 2.** Followup of the C−C and C−H activation reactions of $[Ir(COE)_2Cl]_2$ (**5**) and $[Rh(COE)_2Cl]_2$ (**2a**) with the DTBPM ligand (**1a**) in $C_6D_6$ at 30 °C.

and 2.029(11) Å Rh(Me){2,6-$(CH_2NMe_2)_2C_6H_3$}.[8c]

**Comparison of Different Rhodium Olefin Precursors in the C−C and C−H Bond Activation Processes.** $^{31}P\{^1H\}$ NMR followup of the reaction of **1a** with the cyclooctene complex **2a** revealed the formation of two products: the C−C oxidative addition product **4a** and the C−H activation product **3a**. Initially, parallel formation of the two complexes occurred (**3a:4a** ≈ 1.25:1), but complex **3a** was converted into complex **4a** within several hours (Scheme 2, Figure 2). Only the starting reactants and the products **3a** and **4a** were observed by $^{31}P\{^1H\}$ and $^1H$ NMR throughout the experiment, implying that the olefin substitution in **2a** might be the rate-determining step for the overall reaction (*vide infra*). When the ethylene dimer $[Rh(C_2H_4)_2Cl]_2$ (**2b**) was used, a faster reaction took place and quantitative formation of the C−C and C−H activated complexes **4a** and **3a** was observed already after 15 min at room temperature. The ratio between these complexes was the same as in the reaction with the cyclooctene complex **2a**. No signal due to coordinated ethylene was observed in the $^1H$ NMR spectrum. Upon longer staying in solution at room temperature, complex **3a** was smoothly converted into complex **4a**. These observations indicate that **3a** undergoes slow C−H reductive elimination, followed by rapid metal insertion into the C−C bond. $^{31}P\{^1H\}$ NMR followup showed that the rate of conversion of **3a** into **4a** obeyed first-order kinetics, with $k = 8.59 \times 10^{-5}$ $s^{-1}$, corresponding to $\Delta G^{\ddagger} = 22.4$ kcal/mol.

It is noteworthy that the reaction of ligand **1a** with the rhodium ethylene dimer **2b** is very fast, more than an order of magnitude faster than in the case of the rhodium cyclooctene dimer **2a**. This suggests that the olefin substitution in the latter is, most probably, the rate-determining step for the overall reaction process. Additional evidence for the slow olefin substitution step was obtained from the reaction of the rhodium complex $[Rh(t\text{-}BuC_2H_3)_2Cl]_2$ (**2c**),[9] bearing the bulky *tert*-butylethylene ligands. This reaction was dramatically slower than the reactions of the olefin complexes **2a** and **2b** with **1a**. Moreover, very little (less than 3% according to $^{31}P\{^1H\}$ NMR) of the C−H activation product **3a** was formed at the beginning of the reaction and the C−C activation product was the major complex present in the reaction mixture. $^{31}P\{^1H\}$ NMR followup of this reaction revealed that the disappearance of the free ligand obeyed first-order kinetics with $k = 3.36 \times 10^{-5}$ $s^{-1}$, corresponding to $\Delta G^{\ddagger} = 22.9$ kcal/mol. This value is very close to the one obtained for the C−H reductive elimination from complex **3a**. Thus, buildup of the intermediate (the product of olefin substitution) proceeds with a rate comparable to that of C−H reductive elimination, explaining the fact that only a small amount of **3a** was observed in the reaction between complex **2c** and **1a**.

(9) The synthesis and characterization of the (*tert*-butylethylene)rhodium dimer will be reported elsewhere.

**Scheme 3**

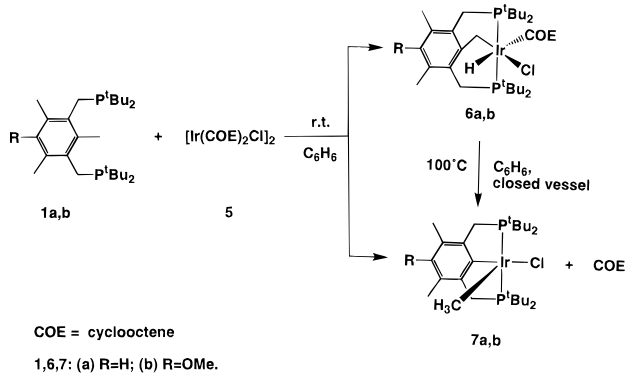


Thus, the increase in the steric bulk of the olefin ligand in the rhodium dimers is responsible for the large decrease in the overall reaction rate. It has been shown that ligand substitution in square-planar $d^8$ transition metal complexes can proceed via an associative mechanism, in which coordination of the incoming ligand precedes ligand dissociation.[10] On the basis of the observed reactivity order of **2b** > **2a** ≫ **2c** we believe that not the C−C and C−H activation steps but rather the *initial coordination of the diphosphine ligand* ***1a*** *to the rhodium olefin complexes is the rate-determining step for the entire process*. The most likely reason for it is the bulkiness of the *tert*-butyl substituents.[11]

**C−C and C−H Bond Activation by Iridium.** When $[Ir(COE)_2Cl]_2$ (**5**, COE = cyclooctene) was reacted with **1a** at room temperature in benzene, parallel formation of two products, the C−H activated complex **6a** and the C−C activated complex **7a**, in an approximate 2:1 ratio was observed (Scheme 3). Due to the different solubility of these complexes in pentane and to the ability to convert **6a** into **7a** (*vide infra*), we were able to isolate and characterize complexes **6a** and **7a** as pure compounds. The $^{31}P\{^1H\}$ NMR spectrum of **6a** exhibits a singlet at 73.95 ppm. $^1H$ and $^{13}C\{^1H\}$ NMR analysis of **6a** reveals that there is no symmetry plane containing the Ir−PCP chelate core. The signal of the methylene Ar−$\mathbf{CH_2}$−Ir group appears as a triplet at 2.09 ppm ($^3J_{PH} = 10.0$ Hz) in $^1H$ NMR and as a triplet at −9.74 ppm ($^2J_{PH} = 5.3$ Hz) in $^{13}C\{^1H\}$ NMR. The hydride signal appears as a triplet at −29.42 ($^2J_{PH,cis} = 11.4$ Hz). $^1H$ and $^{13}C\{^1H\}$ NMR spectra show that cyclooctene is coordinated to the metal and that there is no free cyclooctene in benzene or THF solutions of **6a**. Unambiguous evidence for coordinated cyclooctene in **6a** is the observation that **6a** is converted into **7a** and free cyclooctene at 100 °C. Unlike the related rhodium complex **3a**, complex **6a** is stable in solution at room temperature and does not undergo conversion into **7a** upon heating to 65 °C. This is compatible with the well-known higher stability of iridium alkyl hydrides as compared with rhodium analogs.

The $^{31}P\{^1H\}$ NMR spectrum of **7a** exhibits a singlet at 45.37 ppm. $^1H$ and $^{13}C\{^1H\}$ NMR of this complex demonstrate that there is no symmetry plane passing through the Ir−PCP chelate core. The Ir−$\mathbf{CH_3}$ group of **7a** gives rise to a triplet centered at 1.74 ppm ($^3J_{PH} = 5.0$ Hz) in $^1H$ NMR, the chemical shift being similar to that of the Rh−$\mathbf{CH_3}$ group in **4a** and characteristic for a methyl group *trans* to a vacant coordination

(10) Wilkins, R. G. *Kinetics and Mechanism of Reactions of Transition Metal Complexes*, 2nd ed.; VCH: Weinheim, 1991; p 236.

(11) Low-temperature (−70 °C) $^{31}P\{^1H\}$ NMR followup shows that in the case of the ethylenerhodium dimer **2b** the substitution step is also rate determining for the overall process.

site in five-coordinate square pyramid complexes.[8c,12] In $^{13}C\{^1H\}$ NMR of **7a** the Ir−**CH$_3$** group appears as a triplet at −26.68 ppm ($^2J_{PH}$ = 4.5 Hz). This high-field chemical shift is typical for a methyl group bound to Ir(III).[13] The *cis* orientation of the Ir−**CH$_3$** group with regard to the aromatic ring in **7a** was verified by an NOE experiment, which showed interaction between the Ir−**CH$_3$** group protons and only *one set* of Ar−C***H***$_2$−P and (C***H***$_3$)$_3$C−P protons. Comparison of the splitting pattern of the aromatic carbons in $^{13}C\{^1H\}$ NMR spectra of **6a** and **7a** confirms that in complex **7a** the iridium atom is bound to the aryl ring. Thus, **7a** is a product of *direct insertion* of iridium into the Ar−CH$_3$ bond, analogous to the rhodium complex **4a**. Remarkably, C−C bond activation in our system takes place even at 20 °C. To the best of our knowledge this is the first example of iridium insertion into a strong unstrained C−C bond, which is not driven by aromatization.[14]

When the DIPPM ligand[3b] (**1c**) (2,4-bis[(diisopropylphosphino)methyl]mesitylene, 1,3-bis[(diisopropylphosphino)methyl]-2,4,6-trimethylbenzene), possessing the less bulky isopropylphosphines, was reacted with **5** at room temperature in benzene, C−H and C−C activation took place, but the reaction was not as clean as the one with the DTBPM ligand (**1a**), and formation of side products was observed. Complex **8**, the product of

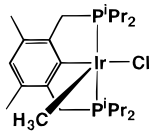


**8**

C−C activation, which gives rise in $^{31}P\{^1H\}$ NMR to a singlet at 39.59 ppm, was purified by chromatography on alumina. The Ir−**CH$_3$** group appears as a triplet at 1.64 ppm ($^3J_{PH}$ = 5.7 Hz) in $^1$H NMR and as a triplet at −32.66 ppm ($^2J_{PH}$ = 4.7 Hz) in $^{13}C\{^1H\}$ NMR. Thus, similarly to **7a**, complex **8** is a product of *direct insertion* of iridium into the Ar−CH$_3$ bond.

**C−C vs C−H Bond Activation. Thermodynamics.** The product of rhodium-promoted C−H activation, **3a**, is *irreversibly* converted into **4a**, the C−C activation product, at room temperature (Scheme 2, Figure 2). Similarly, upon heating in benzene at 100 °C (closed vessel, 0.5 h), the product of C−H bond activation by iridium, complex **6a**, is *irreversibly* converted into the C−C activated product **7a** and free cyclooctene (Scheme 3, Figure 2). This unequivocally proves that the iridium and rhodium insertion into the C−C bond is *thermodynamically more favorable* than their insertion into the C−H bond.

It should be noted that the Ar−CH$_3$ bond in the DTBPM ligand (**1a**) is much stronger than the ArCH$_2$−H bond (compare BDE(C$_6$H$_5$−CH$_3$) = 101.8 ± 2 vs BDE(C$_6$H$_5$CH$_2$−H) = 88 ± 1 kcal mol$^{-1}$ [15]), indicating that the conversion of the C−H activated products into the C−C activated ones (Schemes 2 and 3) is product controlled and that BDE(Ir−Ar + Ir−CH$_3$) > BDE(Ir−CH$_2$Ar + Ir−H + Ir−COE), as well as BDE(Rh−Ar + Rh−CH$_3$) > BDE(Rh−CH$_2$Ar + Rh−H). This is in accordance with the observation that usually the strongest bonds to metals are formed by breaking of the strongest bonds in the substrates.[16] The expected somewhat lower stability of the six-membered chelate ring in the C−H activation complexes, as compared to the five-membered ring in the C−C activation complexes, is also likely to influence their relative stability.

**Table 2.** Ratio between the C−H Activated (**6a**) and C−C Activated (**7a**) Complexes at Different Temperatures in Benzene and THF (by $^{31}P\{^1H\}$ NMR)

| temp, K | C−H:C−C in benzene | C−H:C−C in THF | temp, K | C−H:C−C in benzene | C−H:C−C in THF |
|---|---|---|---|---|---|
| 293 | 100:60 | | 313 | 100:56 | 100:43 |
| 303 | 100:56 | | 323 | 100:56 | 100:46 |
| 305 | | 100:42 | 333 | 100:57 | |

**C−C vs C−H Bond Activation. Kinetics.** Monitoring the reaction of the ligand **1a** with [Ir(COE)$_2$Cl]$_2$ (**5**) by $^{31}P\{^1H\}$ NMR (Figure 2) in benzene in the temperature range of 20−60 °C and in THF at 32−60 °C (the latter was used to probe the solvent effect on the reaction)[17] revealed that *the ratio between the products is constant* at different temperatures during the reaction course and remains the same after the reaction is complete (Table 2; the ratio between **6a** and **7a** is 1.75 ± 0.07 in benzene and 2.29 ± 0.08 in THF). Complexes **6a** and **7a** are formed irreversibly within the temperature range of 20−60 °C, indicating that the C−C and C−H activation processes are *kinetically controlled*, while the constant ratio between **6a** and **7a** demonstrates that the complexes are formed in two *independent concurrent processes*. Thus, the C−H activation product **6a** is not an intermediate in the C−C activation process, which is verified by the observation that it does not convert to **7a** under the reaction conditions. A much higher temperature (100 °C) is required for conversion of **6a** to **7a** (*vide supra*). Initial parallel and temperature independent (within the range 20−40 °C) C−C and C−H activation processes were observed also with rhodium.

The C−C and C−H activation processes are not rate determining in the case of rhodium (*vide supra*) and iridium cyclooctene dimers. In accordance with this, a direct competition experiment, in which equimolar amounts of the rhodium and iridium dimers **2a** and **5** were reacted with a 2-fold excess of **1a**, showed that the reaction rate of the rhodium-promoted activation is about 3 times higher than that of the iridium-promoted one. This is most probably due to the stronger metal−olefin bond in the case of iridium, resulting in slower olefin substitution by the phosphine. We would expect the iridium complex to react faster if either C−C or C−H bond activation were rate determining.

Since both C−C and C−H activation occurs selectively at the methyl group between the two phosphine groups (no other C−H or C−C activated products were observed) precoordination of both phosphine groups to the metal takes place in both activation processes. If C−C activation occurred when only one phosphine is coordinated to the metal center, we would expect formation of stable products (due to the relatively high kinetic barrier of C−C reductive elimination) of activation of all aryl−methyl bonds. Since initial substitution of the olefin ligands with subsequent breaking of the chloride bridge was shown to be a general pathway for the reactions of bulky diphosphines with metal olefin dimers,[18] we believe that the

(12) Fryzuk, M. D.; MacNeil, P.; Rettig, S. J. *Organometallics* **1986**, *5*, 2469.

(13) (a) Mann, B. E.; Taylor, B. F. *$^{13}$C NMR Data for Organometallic Compounds*; Academic Press: New York, 1981. (b) Fryzuk, M. D.; Joshi, K.; Chadha, R. K.; Rettig, S. J. *J. Am. Chem. Soc.* **1991**, *113*, 8724.

(14) C−C bond cleavage of 5,5-dimethylcyclopentadiene to generate a methyliridium cyclopentadienyl complex was reported (see ref 2h).

(15) McMillen, D. F.; Golden, D. M. *Rev. Phys. Chem.* **1982**, *33*, 492.

(16) (a) Bryndza, H. E.; Fong, L. K.; Paciello, R. A.; Tam, W.; Bercaw, J. E. *J. Am. Chem. Soc.* **1987**, *109*, 1444. (b) Nolan, S. P.; Hoff, C. D.; Stoutland, P. O.; Newman, L. J.; Buchanan, J. M.; Bergman, R. G.; Yang, G. K.; Peters, K. S. *J. Am. Chem. Soc.* **1987**, *109*, 3143. (c) Stoutland, P. O.; Bergman, R. G.; Nolan, S. P.; Hoff, C. D. *Polyhedron* **1988**, *7*, 1429.

(17) $^{31}P\{^1H\}$ and $^1$H NMR spectra of a THF-$d_8$ solution of the products of iridium-promoted C−C and C−H activation in THF showed that they are identical to those in benzene (**6a** and **7a**; the analogous complex to **6a** containing coordinated THF is not obtained), which permits the estimation of the solvent effect on the C−C and C−H activation processes.

**Scheme 4**

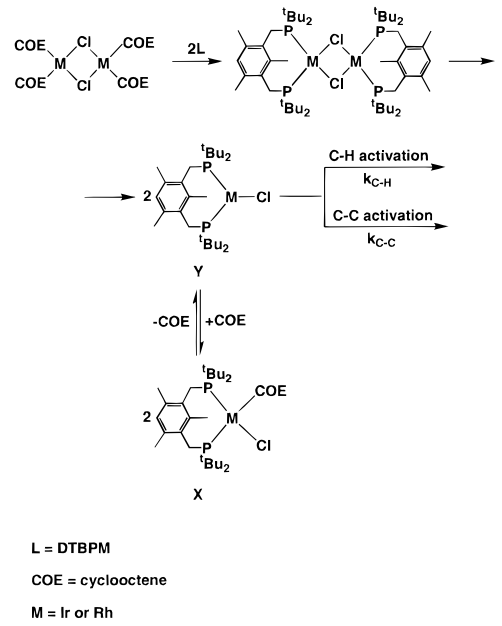


entire reaction leading to C−C and C−H activation proceeds by the route presented in Scheme 4.

The temperature independence of the ratio between the C−C and C−H activation products in the case of iridium and the value of the ratio (C−C:C−H ≈ 1:2) imply that the $\Delta H^{\ddagger}$ and $\Delta S^{\ddagger}$ values for both processes are very similar, indicating that the overall processes leading to C−C and C−H activation proceed by very similar pathways as depicted in Scheme 4.[19] The same arguments apply to the rhodium systems at the beginning of the reaction. The selectivity in the activation processes and similarity of activation parameters for C−H and C−C activation provide very good evidence that *the C−C and C−H activation proceeds via a common intermediate*, and that in this intermediate *the two phosphine arms of the ligand are coordinated to the reactive metal center*. In the case of activation by rhodium the reaction proceeds via the intermediate **Y**, in which the olefin is not coordinated to the metal, since rhodium complexes bearing two bulky phosphine ligands in *trans* configuration are unlikely to coordinate bulky olefins.[20] Significantly, both cyclooctene and ethylene rhodium dimers give the same ratio of C−C and C−H activated products at the beginning of the reaction, indicating that there is no coordinated olefin in the reactive intermediate. However, olefins are known to bind more strongly to iridium, and there is a possibility that the C−C and C−H activation proceeds through intermediate **X** (see Scheme 4) in the case of iridium. Since an excess of free cyclooctene did not affect the ratio between complexes **6a** and **7a**, we believe that the activation reactions in the case of iridium also proceed through a three-coordinate intermediate **Y** analogous to the one proposed for rhodium (Scheme 4). The sterics in **X**, in which cyclooctene is coordinated to iridium, is unfavorable for approaching the "hidden" C−C bond. Moreover, C−C and C−H activation most probably take place *before* COE coordinates to form **X**, due to the expected high reactivity of unsaturated three-coordinate Ir(I) in oxidative addition. Subsequent coordination of cyclooctene to give **6a** takes place, unlike in the case of **7a**, in which it is probably sterically unfavored.

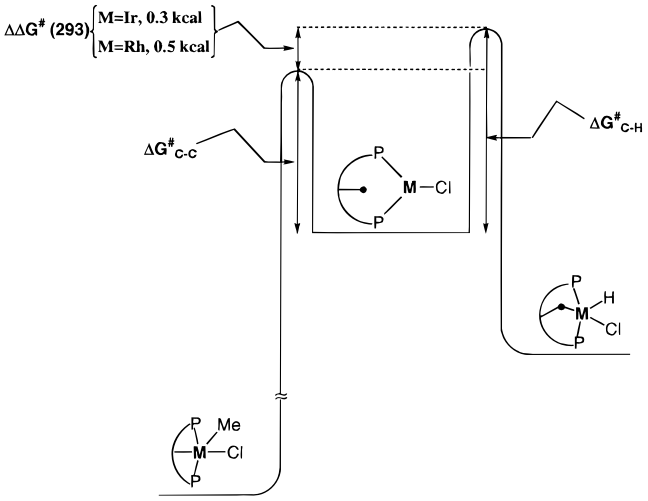


**Figure 3.** Reaction coordinate for C−C and C−H bond activation.

Since the C−C and C−H bond activation occurs in two parallel processes with a *common intermediate*, the ratio between **6a** and **7a** is equal to the ratio between the rate constants of the C−C and C−H activation steps[19] regardless of the rate-determining step of the overall process, i.e., [**6a**]/[**7a**] = $k_{C-H}/k_{C-C}$. The same is true for the rhodium systems at the beginning of the reaction (*vide supra*), i.e., [**3a**]/[**4a**] = $k_{C-H}/k_{C-C}$. Thus, our systems make possible the *direct comparison* between the single C−C and C−H bond activation steps. Taking into account that only one C−C per three C−H bonds is accessible for activation, the calculated ($\Delta\Delta G^{\ddagger}_{12} = -RT \ln(k_1/k_2)$) difference between the free energies of C−H and C−C bond activation is (in benzene) $\Delta\Delta G^{\ddagger}_{CH-CC}(293) = 0.342$ kcal/mol in the case of iridium and $\Delta\Delta G^{\ddagger}_{CH-CC}(293) = 0.501$ kcal/mol in the case of rhodium; i.e., the kinetic barrier for C−H bond activation is about 0.3 kcal/mol (iridium) and 0.5 kcal/mol (rhodium) *higher* than that for C−C activation (see Figure 3).

Surprisingly, *the C−C activation process is both thermodynamically and slightly kinetically more favorable than the C−H bond activation*. The unexpected kinetic preference for C−C activation in our system can be explained by either the specific directionality of the reactive metal orbitals toward the C−C and C−H bonds in the intermediate **Y** or by the interaction of the metal with the $\pi$-system of the aryl ring,[2e,4b] which favors C−C bond cleavage (*vide infra*). It should be noted that the ring strain difference (although expectedly small for five- and six-membered rings) in the transition states associated with the different chelate ring sizes of the C−C and C−H activation products also influences the overall $\Delta\Delta G^{\ddagger}$ value.

On the basis of the temperature independence of the ratio between the iridium C−C and C−H oxidative addition products (and taking into account that one C−C per three C−H bonds is accessible for activation), it follows that $\Delta\Delta H^{\ddagger}_{CH-CC} \approx 0$ kcal/mol and $\Delta\Delta S^{\ddagger}_{CH-CC} = -1.07 \pm 0.05$ eu.

The mechanistic aspects of C−H bond activation by low-valent late transition metals were extensively studied. It was shown that carbon−hydrogen bond breaking involves an early nonpolar three-centered transition state.[1,21] The striking similarity of the activation parameters for C−C and C−H activation processes in the system reported here and the fact that they are not changed much when solvents with different polarities (benzene and THF) are used indicate that *similar nonpolar*

(18) (a) Fryzuk, M. D.; McConville, D. H.; Rettig, S. J. *J. Organomet. Chem.* **1993**, *445*, 245. (b) Hofmann, P.; Meier, C.; Englert, U.; Schmidt, M. U. *Chem. Ber.* **1992**, *125*, 353.

(19) (a) Frost, A. A.; Pearson, R. G. *Kinetics and Mechanism*; John Wiley & Sons: New York, 1961. (b) Laidler, K. J. *Chemical Kinetics*; Harper Collins: New York, 1987.

(20) For example see: Wolf, J.; Lass, R. W.; Manger, M.; Werner, H. *Organometallics* **1995**, *14*, 2649.

(21) Ryabov, A. D. *Chem. Rev.* **1990**, *90*, 403.

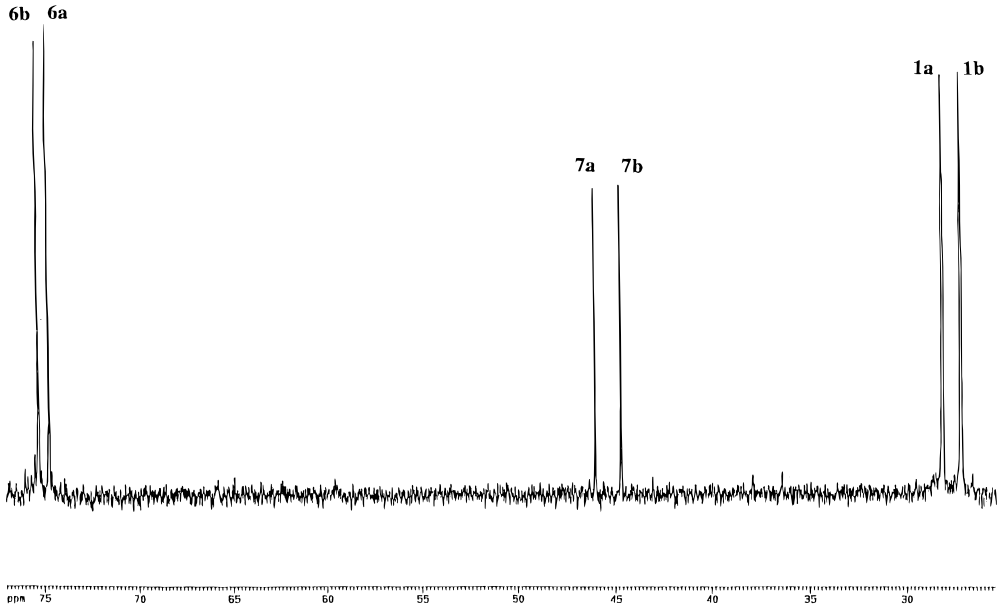


**Figure 4.** $^{31}P\{^{1}H\}$ NMR of a reaction of the ligands **1a** (1 equiv) and **1b** (1 equiv) with $[Ir(COE)_2Cl]_2$ (**5**, 1 equiv) after 0.5 h in $C_6D_6$ at 40 °C.

*transition states* are involved in both processes. The slight preference for C−H activation in THF, as compared to benzene, can be explained by the expected more polar nature of the transition state in the case of C−H activation, which is consistent with the proposed three-centered concerted mechanism.

**C−C and C−H Bond Activation Using A Para-Substituted Ligand.** Further insight into C−C vs C−H bond activation mechanisms was provided by the use of the DTBPA ligand (**1b**), which has a strong electron-donating group in the position para to the carbon−carbon bond to be cleaved. Upon reaction of **1b** with $[Rh(C_2H_4)_2Cl]_2$ (**2b**) (Scheme 2) and with $[Ir(COE)_2Cl]_2$ (**5**) (Scheme 3), complexes **3b** and **6b** (C−H activation products) and **4b** and **7b** (C−C activation products) were formed and unequivocally spectroscopically characterized. The NMR spectra of complexes **3b** and **6b** were almost identical to those of **3a** and **6a**, respectively. Likewise, the NMR spectra of complexes **4b** and **7b** were almost identical to those of **4a** and **7a**, respectively, except for the presence of the signals due to the methoxy group in the DTBPA-based complexes. No changes in the reaction rate or in the products ratio were observed in comparison with **1a**. When **1a** (1 equiv), **1b** (1 equiv), and $[Ir(COE)_2Cl]_2$ (**5**, 1 equiv) were reacted in benzene, parallel formation of **6a** and **6b** as well as **7a** and **7b** was observed, with the ratios **6a:6b** and **7a:7b** being 1:1 (Figure 4). If any charge separation took place at the bond activation stage, we would expect a significant difference in reactivity between **1a** and **1b**.[22] In the case of a nonpolar transition state, influence of substituents in the aryl ring on the reaction rate may also be expected, although it is known to be smaller (kinetic preference of the metal for electron deficient arenes is accounted for in terms of the stronger back-bonding in the metal−arene $\pi$-complex)[23] than in the case of a polar transition state. Thus, the C−C bond cleavage in our system most probably proceeds through *a three-center nonpolar transition state similar to that postulated for C−H bond activation*. Importantly, precoordination to the aryl ring does not seem to be significant for the C−C bond activation.

**Comments on the C−C Activation Mechanism.** Mechanistic information regarding C−C bond activation in solution is lacking. To the best of our knowledge, studies of the intimate mechanism of this important process have not been previously reported.

Our results show that the rhodium and iridium insertion into a nonpolar carbon−carbon bond in the system reported here involves a three-centered concerted process with an early transition state, similar to the one established for the activation of other nonpolar bonds (C−H, Si−H, H−H).[1,2]

High electron density together with coordinative unsaturation should favor C−C oxidative addition, the same as they favor the oxidative addition of other nonpolar bonds. The diphosphine system with the tertiary butyl substituents fits these requirements nicely since the two trialkylphosphine groups bring the metal into the vicinity of the C−C bond to be activated and enhance the electron density on the metal center, while the bulky substituents are capable of shielding a free coordination site and imposing a conformation that favors cyclometalation.[5] Indeed, the C−C activation in the metal−DTBPM and metal−DTBPA systems was achieved under surprisingly mild conditions even though a very strong C−C bond (BDE ≈ 100 kcal/mol) is involved. In the case of the less bulky isopropylphosphines (DIPPM ligand), C−C activation was also observed at room temperature; however, side products were formed as well, probably due to less efficient shielding of the reactive metal center. When the methylphosphine analog of **1a**, 1,3-bis[(dimethylphosphino)methyl]-2,4,6-trimethylbenzene, was reacted with $ClRh(PEt_3)_3$, heating to 150 °C was required in order to achieve C−C oxidative addition, as communicated by us.[4a] This is most probably a result of the much lower steric bulk of the methylphosphine ligands, which permits the formation of a 4-coordinate Rh(I) complex prior to the C−C activation process.

An interesting conclusion is that aromatic ring precoordination, forming an $\eta^2$-arene complex, most probably does not take place in the course of the C−C bond activation in our PCP-based systems. Jones and Feher have demonstrated that formation of an $\eta^2$-arene intermediate precedes the intermolecular C−H bond activation of aromatic hydrocarbons;[24a] this

(22) The electron-donating methoxy substituent is expected to cause significant retardation of a nucleophilic substitution reaction rate when the cleaved bond is in direct polar conjugation to it. For an example of oxidative addition reaction rate correlated with Hammett constants see: Portnoy, M.; Milstein, D. *Organometallics* **1993**, *12*, 1665.

(23) (a) Jones, W. D. In *Activation and Functionalization of Alkenes*; Hill, C. L., Ed.; John Wiley & Sons: New York, 1989; p 111. (b) Selmeczy, A. D.; Jones, W. D.; Osman, R.; Perutz, R. N. *Organometallics* **1995**, *14*, 5677.

was suggested to occur in cyclometalation processes as well, such as in the case of the benzylphosphine ligand in [($C_5Me_5$)Rh($Me_2PCH_2Ph$)].[24b] Involvement of an $\eta^2$-arene complex in the intermolecular cleavage of the C−C bond in the four-membered ring of biphenylene has recently been suggested by Jones et al.[2e] The $\eta^2$-arene complex is generally thought to be an intermediate which brings the metal into the proximity of the C−H or C−C bond to be cleaved. Taking into account that, in the metal−PCP system, the metal center is already held in the vicinity of the carbon−carbon bond by coordination to the two phosphines, aromatic ring precoordination does not seem to be required in the reaction course. A rough estimation based on molecular models shows that formation of the $\pi$-adduct would lead to loss of the symmetry which favors the C−C bond activation, and to steric strain. Similarly, Crabtree et al. showed that $\eta^2$-coordination of the arene to the reactive iridium center does not take place for steric reasons (strain in the chelate ring) in the case of intramolecular C−H activation in 7,8-benzoquinoline.[25]

The observed similarity in activation parameters for the C−H and C−C activation processes is in striking contradiction with the common belief that the barrier for C−C activation is much higher than that of C−H activation.[1c] Theoretical calculations predict that, due to the difference in directionality between bonds to methyl groups and to hydrogen atoms, the activation energy of the C−C bond oxidative addition should be substantially higher (by about 10−20 kcal/mol) than that of the C−H bond.[26] The surprising kinetic preference for the C−C bond activation in our system can be accounted for in terms of the specific directionality of the involved metal orbitals toward the C−C and C−H bonds. It was shown by Crabtree et al. in an investigation of the structures of various agostic compounds that the reaction coordinate of intramolecular C−H bond activation includes rearrangement of a M−H−C species, which is promoted by congested conformations and disfavored in complexes with a lesser degree of congestion (they tend to participate in intermolecular C−H activation).[27] The origin of the surprising kinetic advantage of C−C over C−H activation in our system can be explained in terms of conformation preferences in the reactive intermediate **Y**. We suggest that the kinetic balance between C−H and C−C activation is determined by the configuration of the intermediate, in which the orientation of the metal orbitals involved favors C−C activation. The stability of the products does not seem to play an important role in the kinetics of C−H and C−C activation, since early transition states are involved in both processes.

Interestingly, the kinetic preference for C−C oxidative addition is higher in the case of rhodium than in the case of iridium. This may be due to the higher reactivity of Ir(I) in oxidative addition reactions, resulting in lower selectivity for C−C vs C−H activation.

In this work, C−C oxidative addition to both rhodium and iridium is thermodynamically more favorable than C−H oxidative addition. Although the chelate ring size and the steric bulk of the phosphine ligand are likely to have some influence on the relative stability of the products, we believe that the main factor is electronic. As we have communicated,[4a] reaction of the less bulky *dimethyl*phosphine analog of **1a** yields the more stable C−C activation product, while with the less basic *diphenyl*phosphine analog of **1a** (which is intermediate in size between the *tert*-butyl- and methylphosphine analogs) the C−H activated product is more stable.[3a] Thus, it seems that higher electron density on the metal center thermodynamically favors Ar−$CH_3$ oxidative addition over that of $ArCH_2$−H, perhaps because of the possibility of increased back-bonding into the aromatic $\pi^*$ system in Ar−M, which stabilizes it relative to $ArCH_2$−M. An interesting implication of this observation is that it may be possible to influence the selectivity of thermodynamically controlled C−C vs C−H activation by proper ancillary ligand choice. Significantly, the C−H activation product *is not* an intermediate in the C−C activation process; i.e., direct C−C oxidative addition takes place.

An important result of this work is that there is only a small difference in the kinetic barriers for C−C and C−H bond activation in a system in which late transition metals are brought in a close vicinity of these bonds. Therefore, the *kinetic* reluctance of C−C bonds to insertion of transition metal complexes seems to be predominantly steric in nature. Surrounded by C−H bonds, C−C bonds of hydrocarbons are hidden from the reactive metal center. However, since C−C oxidative addition can be thermodynamically favorable, as demonstrated here, an important question is whether it is possible to bring unstrained unactivated C−C bonds of substrates, which are not bound to a metal via heteroatoms, to close proximity of the metal center in order to achieve intermolecular metal insertion, the entire process being thermodynamically driven.

In conclusion, direct iridium and rhodium insertion into a strong unstrained C−C bond under very mild conditions (room tempreature) in solution was demonstrated. Direct comparison of the C−C and C−H activation processes provided important mechanistic insight into the C−C oxidative addition mechanism. In the systems studied here, the mechanism is similar to that of C−H activation and most probably involves a nonpolar three-centered transition state. $\eta^2$-Arene intermediacy is not involved. Surprisingly, the C−C activation is not only thermodynamically but also slightly kinetically more favorable here than C−H activation, whereas theoretical calculations predict that the activation energy of C−C oxidative addition should be significantly higher than that of C−H bonds. The preference for C−C bond activation is supposedly due to the specific orientation of the relevant metal orbitals toward the C−C bond being cleaved.

## Experimental Section

**General Procedures.** All experiments with metal complexes and phosphine ligands were carried out under an atmosphere of purified nitrogen in a Vacuum Atmospheres glovebox equipped with a MO 40-2 inert gas purifier or using standard Schlenk techniques. All solvents were reagent grade or better. All nondeuterated solvents were refluxed over sodium/benzophenone ketyl and distilled under an argon atmosphere. Deuterated solvents were used as received. All the solvents were degassed with argon and kept in the glovebox over 4 Å molecular sieves. Commercially available reagents were used as received. The complexes $[Rh(COE)_2Cl]_2$,[28] $[Rh(C_2H_4)_2Cl]_2$,[29] and $[Ir(COE)_2Cl]_2$[30] and the phosphine ligand DIPPM[3b] were prepared according to literature procedures.

$^1H$, $^{13}C$, and $^{31}P$ NMR spectra were recorded at 400, 100, and 162 MHz, respectively, using a Bruker AMX-400 NMR spectrometer. All the NMR measurements were performed in $C_6D_6$, unless otherwise specified. $^1H$ NMR and $^{13}C\{^1H\}$ NMR chemical shifts are reported in parts per million downfield from tetramethylsilane. $^1H$ NMR chemical shifts were referenced to the residual hydrogen signal of the deuterated

(24) (a) Jones, W. D.; Feher, F. J. *Acc. Chem. Res.* **1989**, *22*, 91. (b) Jones, W. D.; Feher, F. J. *J. Am. Chem. Soc.* **1985**, *107*, 620.

(25) Lavin, M.; Holt, E. M.; Crabtree, R. H. *Organometallics* **1989**, *8*, 99.

(26) (a) Low, J. J.; Goddard, W. A., III. *J. Am. Chem. Soc.* **1984**, *106*, 10779. (b) Blomberg, M. R. A.; Siegbahn, P. E. M.; Nagashima, U.; Wennerberg, J. *J. Am. Chem. Soc.* **1991**, *113*, 424. (c) Siegbahn, P. E. M.; Blomberg, M. *J. Am. Chem. Soc.* **1992**, *114*, 10548.

(27) Crabtree, R. H.; Holt, E. M.; Lavin, M.; Morenhouse, S. M. *Inorg. Chem.* **1985**, *24*, 1986.

(28) Herde, J. L.; Senoff, C. V. *Inorg. Nucl. Chem. Lett.* **1971**, *7*, 1029.

(29) Cramer, R. *Inorg. Chem.* **1962**, *1*, 722.

(30) Bennett, M. A.; Saxby, J. D. *Inorg. Chem.* **1968**, *7*, 321.

solvents (7.15 ppm, benzene; 3.58 ppm, THF). In $^{13}C\{^1H\}$ NMR measurements the signal of $C_6D_6$ (128.00 ppm) was used as a reference. $^{31}P$ NMR chemical shifts are reported in parts per million downfield from $H_3PO_4$ and referenced to an external 85% solution of phosphoric acid in $D_2O$. Screw-cap 5 mm NMR tubes were used in the NMR followup experiments. Abbreviations used in the description of NMR data are as follows: app, apparent; br, broad; dist, distorted; s, singlet; d, doublet; t, triplet; m, multiplet; v, virtual. Field desorption (FD) mass spectrometry was performed at the University of Amsterdam using a JEOL JMS SX/SX 102A four-sector mass spectrometer, coupled to a JEOL MS-MP7000 data system; mass spectra are reported for the more abundant isotope, namely, $^{193}Ir$. Elemental analyses were performed at the Hebrew University of Jerusalem.

**DTBPM Ligand (1a).** A mixture of di-*tert*-butylphosphine (0.930 g, 6.41 mmol) and 2,6-bis(bromomethyl)mesitylene[6a] (0.914 g, 3.22 mmol) in acetone (5 mL) was heated under reflux with stirring for 40 min to afford a white precipitate. The solid was filtered and washed with ether to remove unreacted starting material. The resulting diphosphonium salt was dissolved in distilled degassed water (10 mL) and treated with a solution of sodium acetate (4 g, 48 mmol) in water (10 mL). The precipitated diphosphine was extracted with ether (3 × 50 mL) and dried over $Na_2SO_4$, and the ether solution was filtered via a sinter tube under argon pressure. The solvent was evaporated under vacuum, giving 1.15 g (82.4%) of the DTBPM ligand as a white solid: $^{31}P\{^1H\}$ NMR 27.07 (s); $^1H$ NMR 6.81 (s, 1H, Ar), 2.86 (d, $^2J_{PH}$ = 2.0 Hz, 4H, Ar−C***H***$_2$−P), 2.84 (s, 3H, C***H***$_3$−Ar), 2.48 (s, 6H, 2 C***H***$_3$−Ar), 1.1 (d, $^3J_{PH}$ = 10.3 Hz, 36H, 4 (C***H***$_3$)$_3$C−P).

**DTBPA Ligand (1b).** 2,6-Bis(bromomethyl)-4-methoxymesitylene was obtained from methoxymesitylene by a known bromomethylation procedure[6a] ($^1H$ NMR ($CDCl_3$) 4.55 (s, 4H, C***H***$_2$Br), 3.66 (s, 3H, OC***H***$_3$), 2.40 (s, 3H, C***H***$_3$), 2.34 (s, 6H, 2 C***H***$_3$)). This compound (0.958 g, 2.85 mmol) and di-*tert*-butylphosphine (0.828 g, 5.67 mmol) were heated with stirring for 40 min under reflux in 5 mL of acetone to afford a white precipitate. The solid was filtered and washed with ether to remove unreacted starting material. The resulting diphosphonium salt was dissolved in distilled degassed water (10 mL) and treated with a solution of sodium acetate (4 g, 48 mmol) in water (10 mL). The precipitated diphosphine was extracted with ether (3 × 50 mL) and dried over $Na_2SO_4$, and the ether solution was filtered via a sinter tube under argon pressure. The solvent was evaporated under vacuum, and the solid was extracted with ether. The ether extract was filtered, and the solvent was evaporated, giving 0.797 g (60%) of the DTBPA ligand as a white solid: $^{31}P\{^1H\}$ NMR 26.86 (s); $^1H$ NMR 3.45 (s, 3H, C***H***$_3$O−Ar), 2.88 (d, $^2J_{PH}$ = 1.8 Hz, 4H, Ar−C***H***$_2$−P), 2.81 (s, 3H, C***H***$_3$−Ar), 2.57 (s, 6H, 2 C***H***$_3$−Ar), 1.10 (d, $^3J_{PH}$ = 10.3 Hz, 36H, 4 (C***H***$_3$)$_3$C−P).

**Reaction of $[Rh(COE)_2Cl]_2$ (2a) with Ligand 1a. Formation of Rh(DTBPM)($CH_3$)Cl (4a).** To a benzene solution (2 mL) of the DTBPM ligand (**1a**) (25 mg, 0.057 mmol) was added 2 mL of a benzene solution of $[Rh(COE)_2Cl]_2$ (**2a**) (20 mg, 0.028 mmol). The mixture was stirred at room temperature for 24 h, resulting in a color change from orange to dark red. $^{31}P\{^1H\}$ NMR revealed quantitative formation of **4a** as a single product. Evaporation of the solvent under vacuum gave complex **4a** as a dark red solid in 98% yield. It is soluble in benzene and THF and moderately soluble in pentane. Single crystals suitable for X-ray diffraction were obtained by crystallization from *n*-hexane at −30 °C.

**Characterization of 4a:** $^{31}P\{^1H\}$ NMR 57.37 (d, $^1J_{RhP}$ = 118.9 Hz); $^1H$ NMR 6.65 (s, 1H, Rh−***Ar***), 2.98 (AB quartet, $^2J_{HH}$ = 17.3 Hz, 4H, Ar−C***H***$_2$−P), 2.22 (s, 6H, 2 Ar−C***H***$_3$), 1.67 (td, $^3J_{PH}$ = 4.9 Hz, $^2J_{RhH}$ = 2.9 Hz, Rh−C***H***$_3$), 1.37 (vt, $J_{PH,virt}$ = 6.4 Hz, 18H, 2 (C***H***$_3$)$_3$C−P), 1.19 (vt, $J_{PH,virt}$ = 6.0 Hz, 18H, 2 (C***H***$_3$)$_3$C−P) (assignment of $^1H$ NMR signals was confirmed by $^1H\{^{31}P\}$ NMR); $^{13}C\{^1H\}$ NMR 168.80 (dt, $^1J_{RhC}$ = 34.0 Hz, $^2J_{PC,cis}$ = 5.9 Hz, $C_{ipso}$, Rh−***Ar***), 146.52 (td, $J_{PC}$ = 8.6 Hz, $J_{RhC} \leq$ 1 Hz, Rh−***Ar***), 130.99 (td, $J_{PC}$ = 8.0 Hz, $J_{RhC}$ = 1.5 Hz, Rh−***Ar***), 127.07 (s, $C_{para}$, Rh−***Ar***), 36.30 (vtd, $J_{PC,virt}$ = 7.1 Hz, $^2J_{RhC}$ = 1.6 Hz, $(CH_3)_3$***C***−P), 36.00 (vt, $J_{PC,virt}$ = 7.5 Hz, $(CH_3)_3$***C***−P), 31.19 (vt, $J_{PC,virt}$ = 2.4 Hz, (***C***H$_3$)$_3$C−P), 30.17 (vtd, $J_{PC,virt}$ = 9.2 Hz, $^2J_{RhC}$ = 2.8 Hz, Ar−***C***H$_2$−P), 29.57 (vt, $J_{PC,virt}$ = 2.0 Hz, (***C***H$_3$)$_3$C−P), 22.31 (s, ***C***H$_3$−Ar), 1.45 (dt, $^1J_{RhC}$ = 30.65 Hz, $^2J_{PC,cis}$ = 5.9 Hz, Rh−***C***H$_3$) (assignment of $^{13}C\{^1H\}$ NMR signals was confirmed by $^{13}C$ DEPT 135). Anal. Calcd: C, 56.46; H, 8.74. Found: C, 56.40; H, 8.77.

**Reaction of $[Rh(ethylene)_2Cl]_2$ (2b) with Ligand 1a. Formation of Complexes Rh(DTBPM)(H)Cl (3a) and 4a.** To a benzene solution (2 mL) of the DTBPM ligand (**1a**) (25 mg, 0.057 mmol) was added 2 mL of a benzene solution of $[Rh(ethylene)_2Cl[_2$ (**2b**) (11 mg, 0.028 mmol). The mixture was stirred at room temperature for 15 min, resulting in a color change from orange to red. $^{31}P\{^1H\}$ NMR revealed quantitative formation of two products, **3a** and **4a** (**3a:4a** = 1.25:1). Upon staying at room temperature for 24 h, complex **3a** was quantitatively converted into **4a**. Complex **3a** was too unstable for isolation and was characterized in solution (mixture, **3a:4a** = 1.25:1). NMR data for **3a**: $^{31}P\{^1H\}$ NMR 101.12 (d, $^1J_{RhP}$ = 139.9 Hz); $^1H$ NMR 6.56 (s, 1H, Ar), 3.15 (AB quartet, $^2J_{HH}$ = 17.2 Hz, 4H, 2 Ar−C***H***$_2$−P), 2.26 (s, 6H, 2 Ar−C***H***$_3$), 2.09 (vtd, $J_{PH,virt}$ = 9.6 Hz, $^2J_{RhH}$ = 3.1 Hz, Rh−C***H***$_2$−Ar), 1.82 (br s, 18H, 2 (C***H***$_3$)$_3$C−P), 1.16 (vt, $J_{PH,virt}$ = 6.1 Hz, 18H, 2 (C***H***$_3$)$_3$C−P), −24.03 (br d, $^1J_{RhH}$ = 13.6 Hz, Rh−***H***) (assignment of $^1H$ NMR signals was confirmed by $^1H\{^{31}P\}$ NMR).

**Reaction of $[Rh(ethylene)_2Cl]_2$ (2b) with Ligand 1b. Formation of Complexes Rh(DTBPA)(H)Cl (3b) and Rh(DTBPA)($CH_3$)Cl (4b).** To a benzene solution (2 mL) of DTBPA ligand (**1b**) (26 mg, 0.056 mmol) was added 2 mL of a benzene solution of $[Rh(ethylene)_2Cl]_2$ (**2b**) (11 mg, 0.028 mmol). The mixture was stirred at room temperature for 15 min, resulting in a color change from orange to dark red: $^{31}P\{^1H\}$ NMR revealed quantitative formation of two products, **3b** and **4b** (**3b:4b** = 1.25:1). Upon staying at room temperature for 24 h, complex **3b** underwent quantitative conversion into **4b**. Evaporation of the solvent under vacuum gave complex **4b** as a dark red solid in 96% yield. It is soluble in benzene and THF and is moderately soluble in pentane. NMR data for **3b**: $^{31}P\{^1H\}$ NMR 102.38 (d, $^1J_{RhP}$ = 140.8 Hz); $^1H$ NMR 3.43 (s, 3H, C***H***$_3$O−Ar), 2.97 (AB quartet, $^2J_{HH}$ = 17.0 Hz, 4H, 2 Ar−C***H***$_2$−P), 2.30 (s, 6H, 2 Ar−C***H***$_3$), 2.09 (td, $^3J_{PH}$ = 9.7 Hz, $^2J_{RhH}$ = 3.0 Hz, Ar−C***H***$_2$−Rh), 1.82 (br s, 18H, 2 (C***H***$_3$)$_3$C−P), 1.16 (vt, $J_{PH}$ = 6.0 Hz, 18H, 2 (C***H***$_3$)$_3$C−P), −24.13 (d, $^1J_{RhH}$ = 14.1 Hz, Rh−***H***). NMR data for **4b**: $^{31}P\{^1H\}$ NMR 57.32 (d, $^1J_{RhP}$ = 119.1 Hz); $^1H$ NMR 3.49 (s, 1H, C***H***$_3$O−Ar), 3.02 (AB quartet, $^2J_{HH}$ = 17.2 Hz, 4H, C***H***$_2$−P), 2.31 (s, 6H, 2 Ar−C***H***$_3$), 1.67 (td, 3H, $^3J_{PH}$ = 4.9 Hz, $^2J_{RhH}$ = 2.9 Hz, Rh−C***H***$_3$), 1.38 (vt, $J_{PH,virt}$ = 6.3 Hz, 18H, 2 (C***H***$_3$)$_3$C−P), 1.21 (vt, $J_{PH,virt}$ = 6.0 Hz, 18H, 2 (C***H***$_3$)$_3$C−P).

**Reaction of $[Ir(COE)_2Cl]_2$ (5) with Ligand 1a. Formation of Complexes Ir(DTBPM)(H)(COE)Cl (6a) and Ir(DTBPM)($CH_3$)Cl (7a).** A benzene solution (2 mL) of the DTBPM ligand (**1a**) (29 mg, 0.067 mmol) was added dropwise to 3 mL of a benzene solution of $[Ir(COE)_2Cl]_2$ (**5**) (30 mg, 0.034 mmol). The mixture was stirred at room temperature for 24 h, upon which its color turned from orange to deep red. $^{31}P\{^1H\}$ NMR revealed formation of two products, exhibiting singlets at 73.95 (complex **6a**) and 45.37 ppm (complex **7a**) in a 2:1 ratio, respectively. The solvent was evaporated under vacuum, and the residue was extracted with pentane (4 × 1 mL). The red pentane extract contained **6a** and **7a** in a 1:1 ratio, and the light brown residue (15 mg) was clean Ir(DTBPM)(H)(COE)Cl (**6a**), yield 29%. The compound is soluble in THF and benzene and moderately soluble in pentane. A $C_6D_6$ solution of a mixture of complexes **6a** and **7a** (**6a:7a** = 2:1) obtained as described above was heated in a closed vessel at 100 °C for 40 min, affording, after solvent evaporation under vacuum, Ir(DTBPM)($CH_3$)Cl (**7a**) as a red oil in quantitative yield ($^{31}P\{^1H\}$ NMR). Heating of a $C_6D_6$ solution (0.6 mL) of pure **6a** (8 mg) at 100 °C in a closed vessel for 30−40 min results in its clean quantitative conversion into Ir(DTBPM)($CH_3$)Cl (**7a**) and free cyclooctene. The compound is soluble in common organic solvents.

**Characterization of 6a:** $^{31}P\{^1H\}$ NMR 73.95 (s); $^1H$ NMR 6.50 (s, 1H, Ir−***Ar***), 3.29 (dvt, the left part of an AB pattern, $^2J_{HH}$ = 14.7 Hz, $J_{PH,virt}$ = 3.5 Hz, 2H, Ar−C***H***$_2$−P), 2.72 (br d, the right part of an AB pattern with unresolved PH coupling, 2H, Ar−C***H***$_2$−P), 2.56 (m, 2H, Ir−***COE***), 2.45 (m, 2H, Ir−***COE***), 2.27 (s, 6H, overlapped with the signal at 2.23, 2 C***H***$_3$−Ar), 2.23 (m, 4H, overall integration with the signal at 2.27 is 10H, Ir−***COE***), 2.09 (t, $^3J_{PH}$ = 10.0 Hz, overlapped with the signal at 2.07, Ar−C***H***$_2$−Ir), 2.07 (m, 2H, overall integration with the signal at 2.09 is 4H, Ir−***COE***), 1.99 (m, 2H, Ir−***COE***), 1.73 (br s, 18H, 2 (C***H***$_3$)$_3$C−P), 1.23 (m, 2H, Ir−***COE***), 1.14 (vt (dist), $J_{PH,virt}$ = 6.0 Hz, 18H, 2 (C***H***$_3$)$_3$C−P), −29.42 (t, $J_{PH,cis}$ = 11.4 Hz, 1H, Ir−***H***) (assignment of $^1H$ NMR signals is confirmed by $^1H\{^{31}P\}$ NMR and $^{13}C-^1H$ inverse correlation); $^{13}C\{^1H\}$ NMR 156.08 (t, $J_{PC}$ = 5.6

Hz, ***Ar***−Ir), 131.35 (t, $J_{PC}$ = 2.5 Hz, ***Ar***−Ir), 126.26 (t, $J_{PC}$ = 1.5 Hz, ***Ar***−Ir), 124.21 (br s, $C_{para}$, ***Ar***−Ir), 62.03 (s, Ir−***COE***), 61.48 (s, Ir−***COE***), 40.23 (vt, $J_{PC,virt}$ = 4.2 Hz, $(CH_3)_3$***C***−P), 37.88 (vt, $J_{PC,virt}$ = 8.7 Hz, $(CH_3)_3$***C***−P), 31.57 (br s, $(CH_3)_3$C−P), 30.47 (br s, $(CH_3)_3$C−P), 30.23 (s, Ir−***COE***), 30.08 (s, Ir−***COE***), 29.95 (s, Ir−***COE***), 29.69 (s, Ir−***COE***), 23.30 (vt, $J_{PC,virt}$ = 12.2 Hz, Ar−***C***$H_2$−P), 19.95 (s, ***C***$H_3$−Ar), −9.74 (t, $^2J_{PC,cis}$ = 5.3 Hz, Ar−***C***$H_2$−Ir) (assignment of $^{13}C\{^1H\}$ NMR signals is confirmed by $^{13}C$ DEPT 135 and $^{13}C-^1H$ inverse correlation); FDMS *m*/*z* 664, $M^+$ − M(COE); 110, $M^+$(COE). Due to the lability of the coordinated cyclooctene, satisfactory elemental analysis was not obtained.

**Characterization of 7a:** $^{31}P\{^1H\}$ NMR 45.37 (s); $^1H$ NMR 6.57 (s, 1H, Ir−***Ar***), 3.08 (dvt, the left part of an AB pattern, $^2J_{HH}$ = 17.2 Hz, $J_{PH,virt}$ = 4.4 Hz, 2H, Ar−C***H***$_2$−P), 2.92 (dvt, the right part of an AB pattern, $J_{PH,virt}$ = 3.5 Hz, 2H, Ar−C***H***$_2$−P), 2.26 (s, 6H, 2 C***H***$_3$−Ar), 1.74 (t, $^3J_{PH}$ = 5.0 Hz, 3H, C***H***$_3$−Ir), 1.35 (vt (dist), $J_{PH,virt}$ = 6.4 Hz, 18H, 2 (C***H***$_3$)$_3$C−P), 1.17 (vt (dist), $J_{PH,virt}$ = 6.1 Hz, 18H, 2 (C***H***$_3$)$_3$C−P) (assignment of $^1H$ NMR signals was confirmed by $^1H\{^{31}P\}$ NMR); $^{13}C\{^1H\}$ NMR 152.83 (br s, ***Ar***−Ir), 146.45 (t, $J_{PC}$ = 7.9 Hz, ***Ar***−Ir), 130.11 (t, $J_{PC}$ = 7.1 Hz, ***Ar***−Ir), 126.56 (s, $C_{para}$, ***Ar***−Ir), 37.39 (vt, $J_{PC,virt}$ = 10.9 Hz, $(CH_3)_3$***C***−P), 35.94 (vt, $J_{PC,virt}$ = 9.3 Hz, $(CH_3)_3$***C***−P), 31.13 (vt, $J_{PC,virt}$ = 2.1 Hz, (***C***$H_3)_3$C−P), 30.83 (vt, $J_{PC,virt}$ = 12.3 Hz, Ar−***C***$H_2$−P), 29.52 (vt, $J_{PC,virt}$ = 2.0 Hz, (***C***$H_3)_3$C−P), 22.40 (s, ***C***$H_3$−Ar), −26.68 (t, $^2J_{PC,cis}$ = 4.5 Hz, ***C***$H_3$−Ir) (assignment of $^{13}C-\{^1H\}$ NMR signals was confirmed by $^{31}C$ DEPT 135); FDMS *m*/*z* 664 ($M^+$). Anal. Calcd: C, 48.82; H, 7.59. Found: C, 49.90; H, 7.57.

**$^1$H NOE Difference Experiment ($C_6D_6$).** When the $CH_3$−Ir group signal of **7a** was selectively irradiated, selective enhancement of the methylene proton signal at 2.92 ppm was observed. When the *tert*-butyl proton signal at 1.35 ppm was selectively irradiated, selective enhancement of the methylene proton signal at 2.92 ppm and of the $CH_3$−Ir group signal at 1.74 ppm was observed.

**Attempted Substitution of COE by THF in 6a.** The complex **6a** (12 mg) was dissolved in THF-$d_8$ (0.6 mL), and its NMR was measured. No substitution of COE was observed. Then a THF-$d_8$ solution of **6a** was heated at 65 °C in a closed vessel for 40 min. No change in $^1H$ and $^{31}P\{^1H\}$ NMR was observed. A THF-$d_8$ solution of **6a** did not show any change in $^1H$ and $^{31}P\{^1H\}$ NMR after staying for 24 h at ambient temperature: $^{31}P\{^1H\}$ NMR (THF-$d_8$) 74.29 (s); $^1H$ NMR (THF-$d_8$) 6.28 (s, 1H, Ir−***Ar***), 3.44 (dvt, the left part of an AB pattern, $^2J_{HH}$ = 14.7 Hz, $J_{PH,virt}$ = 3.5 Hz, 2H, Ar−C***H***$_2$−P), 2.87 (br d, the right part of an AB pattern with unresolved PH coupling, 2H, Ar−C***H***$_2$−P), 2.26 (m, 4H, overall integration with the signal at 2.23 is 10H, Ir−***COE***), 2.23 (s, 6H, overlapped with the signal at 2.23, C***H***$_3$−Ar), 2.14 (m, 2H, Ir−***COE***), 1.93 (m, 4H, Ir−***COE***), 1.84 (t, $^3J_{PH}$ = 10.0 Hz, overlapped with the signal at 1.81, Ar−C***H***$_2$−Ir) 1.81 (m, 2H, overall integration with the signal at 1.84 is 4H, Ir−***COE***), 1.76 (vt, $J_{PH,virt}$ = 5.4 Hz, 18H, 2 (C***H***$_3$)$_3$C−P), 1.64 (m, 2H, Ir−***COE***), 1.12 (vt, $J_{PH,virt}$ = 6.0 Hz, 18H, 2 (C***H***$_3$)$_3$C−P), −29.69 (t, $J_{PH,cis}$ = 11.4 Hz, 1H, Ir−***H***).

**Reaction of $[Ir(COE)_2Cl]_2$ (5) with Ligand 1b. Formation of Complexes Ir(DTBPA)(H)(COE)Cl (6b) and Ir(DTBPA)($CH_3$)Cl (7b).** A benzene solution (3 mL) of the DTBPA ligand (**1b**) (32 mg, 0.069 mmol) was added dropwise to 4 mL of a benzene solution of $[Ir(COE)_2Cl]_2$ (**5**) (30 mg, 0.034 mmol). The mixture was stirred at room temperature for 24 h, upon which its color turned from orange to deep red. $^{31}P\{^1H\}$ NMR revealed formation of two products, exhibiting singlets at 74.51 (complex **6b**) and 44.04 ppm (complex **7b**) in a 2:1 ratio, respectively. The solvent was evaporated under vacuum, and the residue was extracted with pentane (4 × 1 mL). The red pentane extract contained **6b** and **7b** in about a 1:1 ratio, and the light brown residue (16 mg) was clean Ir(DTBPA)(H)(COE)Cl (**6b**), yield 29.3%. The compound is soluble in THF and benzene and moderately soluble in pentane. A $C_6D_6$ solution of a mixture of complexes **6a** and **7b** (**6b**:**7b** = 2:1) obtained as described above was heated in a closed vessel at 100 °C for 1 h, affording, after solvent evaporation under vacuum, Ir(DTBPA)($CH_3$)Cl (**7b**) as a red oil in a quantitative yield. Heating of a $C_6D_6$ solution (0.6 mL) of pure **6b** (10 mg) at 100 °C in a closed vessel results in its clean quantitative conversion into Ir(DTBPA)($CH_3$)Cl (**7b**) and free cyclooctene. The compound is soluble in common organic solvents.

**Characterization of 6b:** $^{31}P\{^1H\}$ NMR 74.51 (s); $^1H$ NMR (the integration was performed on $^1H\{^{31}P\}$ NMR signals) 3.45 (s, 3H, C***H***$_3$O−Ar), 3.30 (dvt, the left part of an AB pattern, $^2J_{HH}$ = 14.8 Hz, $J_{PH,virt}$ = 3.6 Hz, 2H, Ar−C***H***$_2$−P), 2.73 (br d, the right part of an AB pattern with unresolved PH coupling, 2H, Ar−C***H***$_2$−P), 2.54 (m, 2H, Ir−***COE***), 2.44 (m, 2H, Ir−***COE***), 2.34 (s, 6H, 2 C***H***$_3$−Ar), 2.24 (m, 4H, Ir−***COE***), 2.09 (m, 2H, overlapped with the signal at 2.04, Ir−***COE***), 2.04 (t, $^3J_{PH}$ = 10.1 Hz, 2H, Ar−C***H***$_2$−Ir), 1.99 (m, 2H, overlapped with the signal at 2.04, Ir−***COE***), 1.73 (br s, 18H, 2 (C***H***$_3$)$_3$C−P), 1.40 (m, 2H, Ir−***COE***), 1.13 (vt (dist), $J_{PH,virt}$ = 6.0 Hz, 18H, 2 (C***H***$_3$)$_3$C−P), −29.44 (t, $^2J_{PH,cis}$ = 11.6 Hz, 1H, Ir−***H***) (assignment of $^1H$ NMR signals was confirmed by $^1H\{^{31}P\}$ NMR); $^{13}C\{^1H\}$ NMR 152.31 (br s, ***Ar***−Ir), 151.91 (t, $J_{PC}$ = 5.7 Hz, ***Ar***−Ir), 127.22 (t, $J_{PC}$ = 2.5 Hz, ***Ar***−Ir), 124.99 (t, $J_{PC}$ = 2.6 Hz, ***Ar***−Ir), 62.01 (s, Ir−***COE***), 61.53 (s, Ir−***COE***), 59.86 (s, ***C***$H_3$O−Ar), 40.32 (vt, $J_{PC,virt}$ = 4.1 Hz, $(CH_3)_3$***C***−P), 37.98 (vt, $J_{PC,virt}$ = 8.8 Hz, $(CH_3)_3$***C***−P), 31.56 (vt, $J_{PC,virt}$ = 2.0 Hz, (***C***$H_3)_3$C−P), 30.46 (br s, (***C***$H_3)_3$C−P), 30.25 (s, Ir−***COE***), 30.09 (s, Ir−***COE***), 29.95 (s, Ir−***COE***), 29.70 (s, Ir−***COE***), 23.60 (vt, $J_{PC,virt}$ = 12.1 Hz, Ar−***C***$H_2$−P), 13.22 (s, ***C***$H_3$−Ar), −10.07 (t, $^2J_{PC,cis}$ = 5.3 Hz, Ar−***C***$H_2$−Ir) (assignment of $^{13}C\{^1H\}$ NMR signals was confirmed by $^{13}C$ DEPT 135).

**Characterization of 7b:** $^{31}P\{^1H\}$ NMR 44.04 (s); $^1H$ NMR 3.56 (s, 3H, C***H***$_3$O−Ar), 3.11 (dvt, the left part of an AB pattern, $^2J_{HH}$ = 17.3 Hz, $J_{PH,virt}$ = 4.4 Hz, 2H, Ar−C***H***$_2$−P), 2.95 (dvt, the right part of an AB pattern, $J_{PH,virt}$ = 3.5 Hz, 2H, Ar−C***H***$_2$−P), 2.34 (s, 6H, 2 C***H***$_3$−Ar), 1.76 (t, $^3J_{PH}$ = 5.0 Hz, 3H, C***H***$_3$−Ir), 1.35 (vt (dist), $J_{PH,virt}$ = 6.3 Hz, 18H, 2 (C***H***$_3$)$_3$C−P), 1.17 (vt (dist), $J_{PH,virt}$ = 6.1 Hz, 18H, 2 (C***H***$_3$)$_3$C−P) (assignment of $^1H$ NMR signals was confirmed by $^1H-\{^{31}P\}$ NMR); $^{13}C\{^1H\}$ NMR 147.09 (t, $J_{PC}$ = 7.9 Hz, ***Ar***−Ir), 146.59 (s, ***Ar***−Ir), 130.29 (s, ***Ar***−Ir), 123.23 (t, $J_{PC}$ = 7.0 Hz, ***Ar***−Ir), 60.25 (s, ***C***$H_3$O−Ar), 37.45 (vt, $J_{PC,virt}$ = 10.9 Hz, $(CH_3)_3$***C***−P), 35.94 (vt, $J_{PC,virt}$ = 9.4 Hz, $(CH_3)_3$***C***−P), 31.43 (t, $J_{PC,virt}$ = 12.4 Hz, Ar−***C***$H_2$−P), 31.07 (vt, $J_{PC,virt}$ = 2.1 Hz, (***C***$H_3)_3$C−P), 29.63 (vt, $J_{PC,virt}$ = 1.9 Hz, (***C***$H_3)_3$C−P), 15.56 (s, ***C***$H_3$−Ar), −26.85 (t, $^2J_{PC,cis}$ = 5.0 Hz, ***C***$H_3$−Ir) (assignment of $^{13}C\{^1H\}$ NMR signals was confirmed by $^{31}C$ DEPT 135); FDMS *m*/*z* 694, $M^+$.

**Ir(DIPPM)($CH_3$)(Cl) (8).** A benzene solution (3 mL) of the DIPPM ligand (**1c**) (54 mg, 0.142 mmol) was added dropwise to 4 mL of a benzene solution of $[Ir(COE)_2Cl]_2$ (**5**) (65 mg, 0.073 mmol). After 3 h of stirring at ambient temperature, the initial orange color of the mixture turned deep red-violet. The $^{31}P\{^1H\}$ NMR spectrum of the reaction mixture revealed formation of three major products appearing as singlets at 62.15 ppm (doublet in hydride coupled $^{31}P$ NMR, the product of C−H activation), 39.59 ppm (complex **8**, the product of C−C activation), and 28.46 ppm. The C−H activated complex was not isolated from the reaction mixture. Selected NMR data of this complex: $^{31}P\{^1H\}$ hydride coupled NMR ($C_6D_6$) 62.15 (d, $J_{PH,cis}$ = 15.0 Hz); $^1H$ NMR ($C_6D_6$) −28.95 (t, $^2J_{PH,cis}$ = 15.0 Hz).

The reaction was monitored by $^{31}P\{^1H\}$ NMR at ambient temperature, which revealed that the ratio between the products *is not constant* during the reaction course. The mixture was stirred for 24 h at ambient temperature and then heated for 24 h in a closed vessel at 85−90 °C. $^{31}P\{^1H\}$ NMR revealed preferential formation of two products (singlets at 39.59 and 28.45 ppm) in a 1:1 ratio. The solvent was evaporated under vacuum, and the residue was extracted with pentane. Both products were soluble in pentane. The pentane extract was passed through a small column (Pasteur pipet) packed with alumina II−III, and the red residue was washed on the column with 5 mL of pentane and then eluted with a pentane/THF (20:1, v/v) mixture. The red band was collected, yielding 23 mg (26.7%) of clean **8** as an oil of deep red-violet color. The compound is soluble in common organic solvents.

**Characterization of 8:** $^{31}P\{^1H\}$ NMR 39.59 (s); $^1H$ NMR 6.59 (s, 1H, Ir−***Ar***), 2.90 (dvt, the left part of an AB pattern, $^2J_{HH}$ = 17.5 Hz, $J_{PH,virt}$ = 4.6 hz, 2H, Ar−C***H***$_2$−P), 2.79 (dvt, the right part of an AB pattern, $J_{PH,virt}$ = 4.0 Hz, 2H, Ar−C***H***$_2$−P), 2.59 (m, 2H, $(CH_3)_2$C***H***−P), 2.23 (s, 6H, 2 C***H***$_3$−Ar), 2.14 (m, 2H, $(CH_3)_2$C***H***−P), 1.64 (t, $^3J_{PH,cis}$ = 5.7 Hz, 3H, C***H***$_3$−Ir), 1.35 (app quartet, $J$ = 7.3 Hz, 6H, (C***H***$_3)_2$-CH−P), 1.25 (app quartet, $J$ = 7.3 Hz, 6H, (C***H***$_3)_2$CH−P), 1.15 (app quartet, $J$ = 7.1 Hz, 6H, (C***H***$_3)_2$CH−P), 0.87 (app quartet, $J$ = 7.1 Hz, 6H, (C***H***$_3)_2$CH−P) (assignment of $^1H$ NMR signals was confirmed by $^1H\{^{31}P\}$ NMR); $^{13}C\{^1H\}$ NMR 150.13 (br s, ***Ar***−Ir), 145.87 (t, $J_{PC}$ = 8.8 Hz, ***Ar***−Ir), 130.45 (t, $J_{PC}$ = 7.4 Hz, ***Ar***−Ir), 126.64 (s, $C_{para}$, ***Ar***−

Ir), 32.35 (vt, $J_{PC,virt}$ = 15.0 Hz, Ar−***C***$H_2$−P), 27.20 (vt, $J_{PC,virt}$ = 13.4 Hz, $(CH_3)_2$***C***H−P), 23.91 (vt, $J_{PC,virt}$ = 13.8 Hz, $(CH_3)_2$***C***H−P), 22.38 (s, ***C***$H_3$−Ar), 19.64 (s, (***C***$H_3)_2$CH−P), 19.46 (s, (***C***$H_3)_2$CH−P), 18.71 (br s, (***C***$H_3)_2$CH−P), 17.70 (s, (***C***$H_3)_2$CH−P), −32.66 (t, $J_{PC}$ = 4.7 Hz, ***C***$H_3$−Ir) (assignment of $^{13}C\{^1H\}$ NMR signals was confirmed by $^{13}C$ DEPT 135); FDMS *m*/*z* 608, $M^+$. Anal. Calcd: C, 45.42; H, 6.96. Found: C, 46.85; H, 6.97.

**X-ray Analysis of the Structure of 4a.** Complex **4a** was recrystallized from hexane at −30 °C to give orange crystals. The overall $I/\sigma(I)$ for data was 7.5, and many reflections were with split profiles.

**Crystal Data.** $C_{27}H_{50}P_2ClRh$, orange plates, 0.2 × 0.2 × 0.1 $mm^3$, monoclinic, $P2_1/c$ (no. 14), $a$ = 12.282(2) Å, $b$ = 15.682(3) Å, $c$ = 15.996(3) Å, $\alpha = \gamma = 90°$, $\beta$ = 111.47(3)°, from 25 reflections, $T$ = 110 K, $V$ = 2867.1(9) $Å^3$, $Z$ = 4, FW = 547.97, $D_c$ = 1.332 $Mg/m^3$, $\mu$ = 0.813 $mm^{-1}$.

**Data Collection and Treatment.** Rigaku AFC5R four-circle diffractometer, Mo Kα, graphite monochromator ($\lambda$ = 0.710 73 Å). Data were collected to $2\theta = 42°$ only, as the diffraction was very weak beyond this limit. A total of 5825 reflections collected, $1.78° \le \theta \le 21.00°$, $-12 \le h \le 12$, $0 \le k \le 15$, $-16 \le l \le 11$, $\omega$ scan method, scan width 1.6°, scan speed 6°/min, and typical half-height peak width 0.45°. Three standards were collected 28 times each, with a 4% change in intensity, 3081 independent reflections ($R$-int = 0.0588).

**Solution and Refinement.** The structure was solved by the Patterson method (SHELXS-92). Full-matrix least-squares refinement was based on $F^2$ (SHELXL-93). Idealized hydrogens were placed and refined in a riding mode, 293 parameters with 32 restraints (C−C bond distances and angles in tertiary butyl groups), final $R_1$ = 0.1052 (based on $F^2$) for data with $I > 2\sigma(I)$ based on 2574 reflections and $R_1$ = 0.1617 for all data, goodness-of-fit on $F^2$ = 1.140, largest electron density 1.594 e/$Å^{-3}$.

There is large thermal motion on the tertiary butyl groups, but they have not been modeled as discretely disordered. As the crystal was frozen in an oil droplet, neither an explicit nor empirical absorption correction was done.

**NMR Followup Experiments. NMR Measurements and Data Processing.** The processes were monitored by $^{31}P\{^1H\}$ NMR. The spectra were measured using 5 mm screw-cap NMR tubes, which were inserted into the NMR spectrometer probe preset at the desired temperature. The monitoring program was started after 2−3 min of temperature equilibration and included periodical FID acquisition at constant intervals. The delay was varied in different experiments from 5 to 30 min, depending on experimental conditions. The reactions were monitored until completed. The spectra were processed (Fourier-transform, baseline, and phase correction, integration) using an automatic program. Raw data from the spectra were processed using the Cricket Graph program on a Macintosh personal computer.

**(a) Reaction of the DTBPM Ligand (1a) with $[Rh(COE)_2Cl]_2$ (2a).** In a typical experiment 0.5 mL of a benzene solution of **2a** (8 mg, 0.011 mmol) was added to a solution of 10 mg (0.023 mmol) of **1a** in 0.5 mL of benzene. The followup measurements were performed at 20, 30, and 40 °C.

**(b) Reaction of the DTBPM Ligand (1a) with $[Rh(tBuC_2H_3)_2Cl]_2$ (2c).** In a typical experiment 0.5 mL of a benzene solution of **2c** (5 mg, 0.011 mmol) was added to a solution of 10 mg (0.023 mmol) of **1a** in 0.5 mL of benzene. The followup measurements were performed at 20 °C.

**(c) Reaction of the DTBPM Ligand (1a) with $[Ir(COE)_2Cl]_2$ (5).** In a typical procedure complex **5** (30 mg, 0.034 mmol) and **1a** (29 mg, 0.067 mmol) were dissolved in a mixture of $C_6D_6$ (1.5 mL) and $C_6H_6$ (2 mL) or in 4 mL of THF. The followup measurements were performed at 20, 30, 40, 50, and 60 °C in the case of benzene and at 32, 40, and 50 °C in the case of THF.

**(d) Reaction of DTBPM (1a) and DTBPA (1b) Ligands with $[Ir(COE)_2Cl]_2$ (5) (Competition Experiment).** In a typical procedure **5** (27 mg, 0.030 mmol), **1a** (14 mg, 0.030 mmol), and **1b** (13 mg, 0.030 mmol) were dissolved in a mixture of $C_6D_6$ (1 mL) and $C_6H_6$ (1 mL). The followup measurements were performed at 40 and 50 °C.

**(e) Reaction of the DTBPM Ligand (1a) with $[Ir(COE)_2Cl]_2$ (5) and $[Rh(COE)_2Cl]_2$ (2a) (Competition Experiment).** In a typical procedure **5** (10 mg, 0.011 mmol), **2a** (8 mg, 0.011 mmol), and **1a** (50 mg, 0.114 mmol) were dissolved in a mixture of $C_6D_6$ (1 mL) and $C_6H_6$ (1 mL). The followup measurements were performed at 30 °C.

**Acknowledgment.** We thank Dr. Michael Aizenberg and Dr. Ofer Blum for valuable discussions and Dr. Linda J. W. Shimon for performing the X-ray structural analysis. This work was supported by the Israel Science Foundation, Jerusalem, Israel, and by the U.S. − Israel Binational Science Foundation, Jerusalem. A.V. thanks the Ministry of Science and the Arts, Jerusalem, for a fellowship. D.M. is the holder of the Israel Matz professorial chair of organic chemistry.

**Supporting Information Available:** Tables of crystal data and structure refinement, atomic coordinates, bond lengths and angles, anisotropic displacement parameters, and hydrogen atom coordinates for complex **4a** (8 pages). See any current masthead page for ordering and Internet access instructions.

JA962253R